OCTOBER 1975 MATT-1152

IMPURITY TRANSPORT IN A QUIESCENT TOKAMAK PLASMA

BY

S. A. COHEN, J. L. CECCHI,
AND E. S. MARMAR

PLASMA PHYSICS LABORATORY

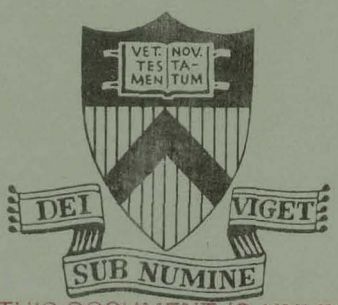

PRINCETON UNIVERSITY
PRINCETON, NEW JERSEY

This work was supported by U. S. Energy Research and Development Administration Contract E(11-1)-3073. Reproduction, translation, publication, use and disposal, in whole or in part, by or for the United States Government is permitted.

DISCLAIMER

NOTICE

Printed in the United States of America.

Available from
National Technical Information Service
U. S. Department of Commerce
5285 Port Royal Road
Springfield, Virginia 22151
Price: Printed Copy $ *; Microfiche $1.45

*Pages	NTIS Selling Price
1-50	$ 4.00
51-150	5.45
151-325	7.60
326-500	10.60
501-1000	13.60

Impurity Transport in a Quiescent Tokamak Plasma

S. A. Cohen, J. L. Cecchi
and E. S. Marmar

Plasma Physics Laboratory, Princeton University
Princeton, New Jersey 08540

ABSTRACT

We have injected short bursts of aluminum into the Adiabatic Toroidal Compressor (ATC) Tokamak, and measured the time evolution of the radial distributions of highly ionized states of aluminum. The results are compared with a computer code describing neoclassical impurity diffusion and good agreement is found.

The transport of high - Z ions in tokamak plasmas is of crucial importance because impurity profiles greatly affect radiation losses[1], reactivity[2] and stability[3], as well as the efficiency of the various heating schemes[4]. Considerable efforts have been made to measure intrinsic impurity content[5,6] and profiles[7,8]. However, it is difficult to determine transport coefficients from these experiments because of the lack of knowledge of the impurity source function. Recent attempts to circumvent this problem by using pulsed gas methods[8,9] have suffered from other problems. These have been previously discussed[10]. By employing a new impurity injection technique[10] in conjunction with vacuum ultra-violet (VUV) spectroscopy, we have been able to measure the radial transport of aluminum ions in a dirty ($Z_{eff} \approx 4.6$), quiescent (no large kink-like modes), tokamak plasma. The measurements have been compared with a computer code describing Pfirsch-Schlüter impurity diffusion and good agreement is found. We consider this to be further evidence of the neoclassical behavior of ions in tokamaks.

The details of the impurity injection technique have been described elsewhere[10]. High power laser irradiation of an aluminized glass slide produces a 300 μsec burst containing $\sim 5 \times 10^{16}$ neutral aluminum atoms with ~3 eV mean energy. These atoms are directed into the Adiabatic Toroidal Compressor (ATC) Tokamak, in which the total number of electrons is approximately 10^{19}. The injected aluminum atoms penetrate about 2 cm into the plasma before being ionized to Al II. The ionization process

continues as the ions rapidly circulate along the field lines and, less rapidly, move across them. The time evolution of the line integral of the emissivity for different aluminum ionization states is measured using an absolutely calibrated, grazing incidence VUV monochrometer (MacPherson model 247) The monochrometer may be scanned across different chords of ATC. Observations are made of the strong $\Delta n = 0$ transitions to the ground state. The observed transitions are listed in Table I.

During these experiments magnetic probes showed that no large MHD kink-like modes were present and that the up-down and in-out stability was ±1.0 cm. Using a 4mm microwave interferometer the average electron density, $\langle n_e \rangle$, was measured. Within 4 ms after aluminum injection $\langle n_e \rangle$ increased 5% above the no-injection case. The 5% increase is consistent with the amount of aluminum injected. This change in $\langle n_e \rangle$ decayed with a 7 ms time constant. However, Thomson scattering measurements of the electron temperature and density profiles showed no discernible changes, i.e., $\frac{\Delta T_e}{T_e}$, $\frac{\Delta n_e}{n_e} \leq 0.1$, hence it was not possible to determine if either the increase or decay of $\langle n_e \rangle$ was due to a change in the total number of electrons or to a change in the n_e profile. The peak electron density and temperature were $2.5 \times 10^{13} cm^{-3}$ and 1400 eV respectively; the electron density radial profile is approximately parabolic. The safety factor, q(r), computed from the Thomson scattering data[11], was 0.6, 1.0 and 3.0 at r = 0, 7 and 17 cm

respectively. Z_{eff}, also computed from the Thomson scattering data, was 4.6. Most of this is accounted for by the measured oxygen concentration in the plasma. However, measurements of the radial distribution of the total oxygen density is not possible by UV techniques because most of it is fully stripped. The peak proton temperature was approximately 180 eV. Profiles of proton temperature and density have not been measured in ATC; however, measurements on ST[12] and ORMAK[13], as well as computer simulations[14] for ATC, show nearly parabolic proton temperature and density profiles.

After injection, observations of different Al ionization states were made along chords of the minor cross section. These were Abel inverted and the impurity density was unfolded from the photon signals in the usual manner. The salient feature of the results is that each ionization state appears in a particular cylindrical shell of the plasma. The density of a particular ionization state increases in time, then decreases, but does not discernably move from its shell. The normalized radial distributions of three adjacent ionization states, Al IX, X, and XI, are shown in Fig. 1. The error bar for the radial coordinate is primarily due to uncertainty in the absolute up-down position of the plasma; the error bar for the density coordinate is due to the statistics of the measurement. The time evolution for the normalized line integral (across the minor diameter) of

photon signals from 5 consecutive ionization states is shown in Fig. 2a. The t = 0 point represents the time at which the aluminum neutrals entered the plasma. The time constant of the detection system was 200 μsec. Each trace represents the average of 5 pulses. These three measurements -- the radial profiles, the time evolutions and the peak absolute brightnesses -- form a complete description of aluminum transport in the region 8 to 14 cm. (A study of transport inside r = 8 cm using soft x ray techniques to observe Al XII is underway.)

To compare these results with theory we have developed a one-dimensional computer code that describes impurity diffusion in the Pfirsch-Schlüter regime. This code numerically integrates the following set of coupled equations

$$\frac{\partial n_j}{\partial t} = \frac{-1}{r} \frac{\partial}{\partial r} (r\Gamma_j) + S_j \qquad j = 1, 13 \qquad (1)$$

with the flux of the j^{th} ionization state given by[15]

$$\Gamma_j = \sum_b \frac{\rho_b^2 Z_b \nu_{bj}}{Z_j T_b} (1+\alpha_1 q^2) \left[T_b \frac{\partial n_b}{\partial r} - \frac{n_b}{n_j} \frac{Z_b}{Z_j} T_j \frac{\partial n_j}{\partial r} \right], \qquad (2)$$

where

n_j = density of the j^{th} state of ionization of aluminum: eg., j = 5 for Al VI,

b = background ions (oxygen and hydrogen)

ρ_b = Larmor radius for the background ion species = $\frac{(2m_b T_b)^{1/2}}{Z_b eB}$,

Z_b = charge state of background ions,

T_b = temperature of background ions,

ν_{bj} = collision frequency of background ions with aluminum = $4(2\pi)^{1/2} n_j Z_j^2 Z_b^2 e^4 \ell n\Lambda / 3 m_{ab}^{1/2} T_b^{3/2}$

m_{ab} = reduced mass

n_b = density of the background ions,

S_j = source terms for the $j^{\underline{th}}$ ionization state. These include electron impact ionization[16], dielectronic[17] and radiative[18] recombination, and

α_1 = a constant of order unity[15].

We have calculated that diffusion caused by collisions between different Al ionization states, as well as temperature gradient contributions are negligible. In the code we specify that there is no recycling of Al lost at the edge. The different ion species are assumed to have temperatures equal to the local proton temperature. The electron and proton density profiles are assumed to be stationary in time and to have equal logarithimic spatial derivatives given by the measured electron profile. The absolute concentrations of oxygen is set so that $Z_{eff} = 4.6$ on axis. The oxygen ionization states are determined from coronal equilibrium in the region r = 0 to 14 cm. Outside this volume the oxygen is assumed to be five times ionized. The initial distribution of Al II was calculated from the measured energy distribution of the injected neutrals[10] and the measured electron temperature and density profiles of ATC.

account in the computer code source function. However, the spreading in time of the particles along the field lines to the azimuthal position of the monochrometer was not included since the interval is smaller than the experimental uncertainties.

The results of the code are in good agreement with the experiment. The code does predict the "stationary shell" effect. The insert in fig. 1 shows the code predictions for the radial location (RL) and the width (FWHM) of Al IX, X, and XI. Figures 2b and 3b show the predicted time evolution and absolute brightness for the observed line of each state. In all, only the brightness of Al XI does not give good agreement.

The uncertainties in comparing the code with the experiment must be stressed. First, the inward diffusional flux of aluminum caused by the oxygen gradient is about 2-3 times that caused by the proton gradient, and the oxygen profile is the least accurately known quantity. However, if the oxygen gradient is any steeper than we have assumed, the diffusion must be slower than neoclassical, and if the oxygen gradient is less steep than assumed, then the diffusion can be at most 3 times greater than neoclassical. The predictions of the code are insensitive to errors in either the recombination rate coefficients up to a factor of 30 for the states Al V to Al XI, or the ionization rate coefficients up to a factor of 1.5. We have also investigated the effects on the code of varying the proton and electron temperatures. Taking into account all the stated uncertainties we infer that the diffusion coefficient is within a factor of 3 of the theoretical (see eq. 1).

Groups at ORMAK[19], T-4[20] and ATC[14] have investigated ion thermal conductivity and found it to be neoclassical. Groups at T-3[7] and ATC[8] have investigated impurity transport and conclude that it is inward. The present work also reports inward diffusion with a transport coefficient close to neoclassical. However, x ray experiments on ST[9] have shown no peaking of the impurity profile on axis. We stress that our transport studies were performed in the region outside the $q = 1$ surface. It is possible that transport inside this region is turbulent and hence peaking of the impurity profile is avoided.

ACKNOWLEDGMENTS

We wish to thank H. P. Furth, R. J. Goldston, E. Mazzucato, and P. H. Rutherford for useful discussions; C. C. Daughney for providing the Thomson scattering data, and R. Shoemaker and R. Moore for their able technical assistance.

This work was supported by United States Energy Research and Development Administration (formerly AEC) Contract AT(11-1)-3073.

[1] D. M. Meade, Nucl. Fusion 14, 289, (1974).

[2] D. L. Jassby, TM-274, (1974).

[3] D. W. Ross, Nucl. Fusion 14, 447, (1974).

[4] J. P. Girard, D. Marty and P. Moriette, 5th Int. Conf. on Plasma Physics and Controlled Thermonuclear Fusion Research (TOKYO 1974), Paper A17-2.

[5] E. Hinnov, et al, MATT-251, (1964).

[6] F. DeMarco, MATT-1012, (1973).

[7] V. I. Gervids and V. A. Krupin, ZhETF Pis. Red. 18, 106, (1973).

[8] J. L. Cecchi, Bull. Amer. Phys. Soc. 19, 853, (1974).

[9] S. von Goeler, et al, Nucl. Fusion 15, 301, (1975).

[10] E. S. Marmar, J. L. Cecchi, and S. A. Cohen, Rev. Sci. Instru. 46, (1975).

[11] C. C. Daughney, MATT-1118, (1975).

[12] D. Dimock, et al., Plasma Physics and Controlled Nuclear Fusion Research, Proc. 4th Int. Conf., Madison, U.S.A., 1971, 1 IAEA, VIENNA, (1971), 451.

[13] J. Lyon, private communications.

[14] P. H. Rutherford, private communications; and P. E. Stott, MATT-1116, (1975).

[15] P. H. Rutherford, Phys. Fluids, 17, 1782, (1974).

[16] W. Lotz, Institut für Plasmaphysik, Garching bie München, IPP 1/62, (1967).

[17] W. Huebner, A. Merts, and B. Cowan, private communication.

[18] R. C. Elton, Methods of Experimental Physics, 9, Pt. A, H. R. Griem and R. H. Lovberg, eds. (Academic, New York, 1970).

[19] L. A. Berry, J. F. Clarke, and J. T. Hogan, Phys. Rev. Lett., 32, 362, (1974).

[20] E. P. Gorbunov, V. S. Zaverjaev, and M. P. Petrov, 6th European Conf. on Controlled Fusion and Plasma Physics (Joint Institute for Nuclear Research, MOSCOW, 1973) 1, 1.

TABLE I - Observed Aluminum Transitions

Ionization State	Transition	Wavelength (A^o)
V	$2s^2 2p^5 (^3P^o_{1/2}) - 2s2p^6 (^2S_{1/2})$	278.7
VI	$2s^2 2p^4 (^3P_2) - 2s2p^5 (^3P^o_2)$	309.6
VII	$2s^2 2p^3 (^4S^o_{3/2}) - 2s2p^4 (^4P_{1/2})$	352.2
VIII	$2s^2 2p^2 (^3P_2) - 2s2p^3 (^3D^o_3)$	388.0
IX	$2s^2 2p (^2P^o_{1/2}) - 2s2p^2 (^2D_{3/2})$	385.0
X	$2s^2 (^1S_o) - 2s2p (^1P^o_1)$	332.8
XI	$2s (^2S_{1/2}) - 2p (^2P^o_{3/2})$	550.0

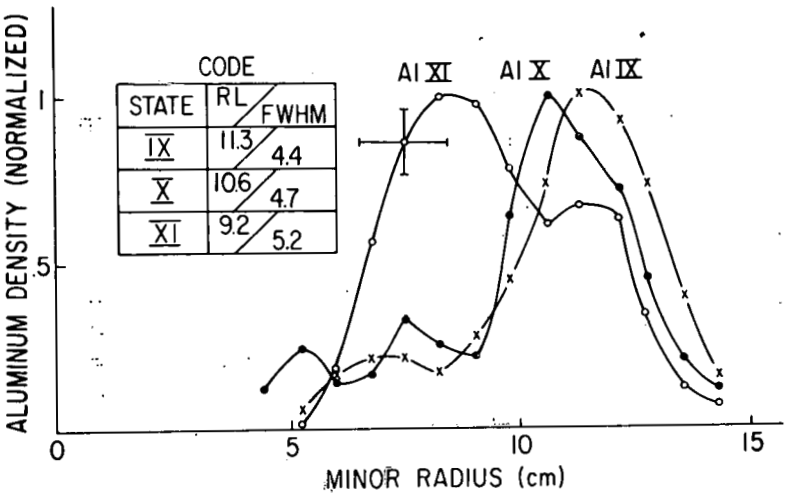

753557

Fig. 1. Radial Distributions of Al IX, X and XI measured at the time of their peak intensity. The insert shows the calculated radial positions (RL) and full width - half maximums (FWHM) for the same states.

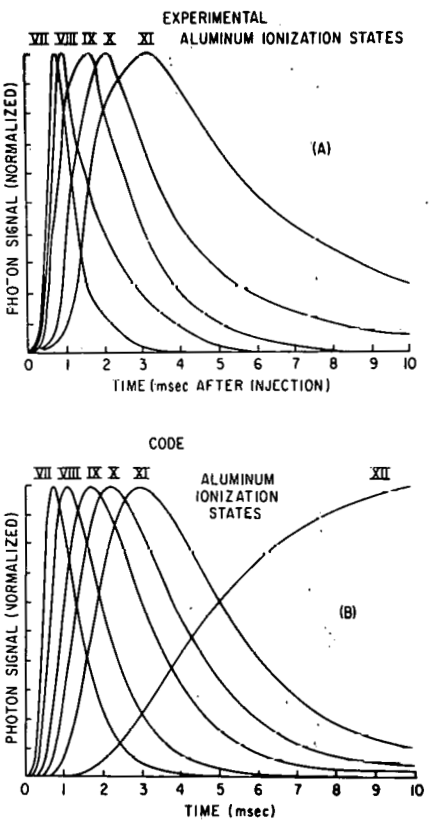

753553

Fig. 2. Time evolution of the normalized line integral Al photon signals. (A) experimental; (B) calculated.

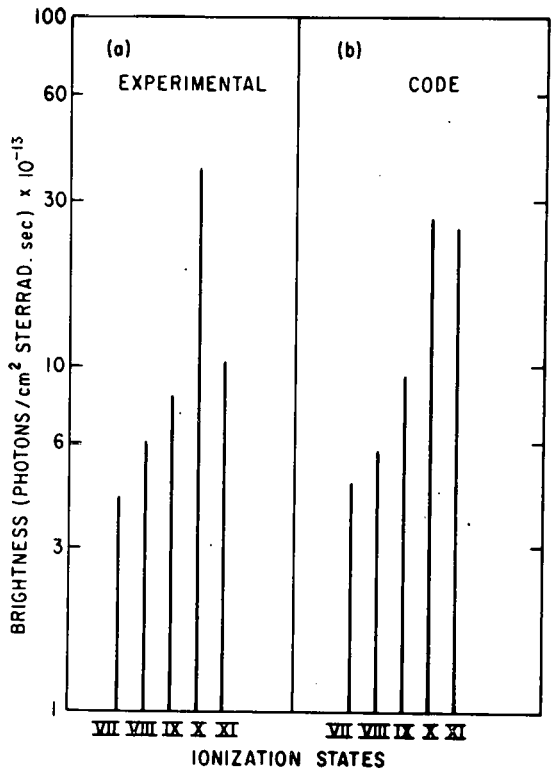

753554

Fig. 3. Absolute peak brightness of Al lines. (a) experimental; (b) calculated.